

## **Aerodynamic Simulation, Thermal and Fuel Consumption Analysis of Hydrogen Powered Fuel Cell Vehicle**

**Ajay Kumar<sup>a</sup>, Sachin Mishra, Brajesh Tripathi, Pradeep Kumar and Ish Hunar Sharma**

*Gautam Buddha University, Greater Noida, India*  
*<sup>a</sup>Corresponding Author, Email: [ajaygbu@gmail.com](mailto:ajaygbu@gmail.com)*

### **ABSTRACT:**

*This paper presents design, analysis and development of a highly aerodynamic and a near zero emission single seater three wheeler unfrozen hawk prototype vehicle that is powered by hydrogen fuel cell. The vehicle is designed with a tadpole configuration and gullwing doors to achieve low drag and a streamlined half body. The pressure and velocity distribution with an optimal value of drag coefficient are established using computational fluid dynamic analysis. The hydrogen consumption and heat generated in the fuel cell & brushless direct current motor are analyzed for various cases. The study concluded to show a reduction in power and fuel consumption of designed prototype vehicle to give better fuel economy and overall performance.*

### **KEYWORDS:**

*Fuel cell vehicle; Computational fluid dynamics; Gullwing door; Tadpole three-wheeler; Thermal performance*

### **CITATION:**

A. Kumar, S. Mishra, B. Tripathi, P. Kumar and I.H. Sharma. 2015. Aerodynamic Simulation, Thermal and Fuel Consumption Analysis of Hydrogen Powered Fuel Cell Vehicle, *Int. J. Vehicle Structures & Systems*, 7(1), 31-35. doi:10.4273/ijvss.7.1.06.

## **1. Introduction**

The green vehicles have to be equipped with a low and limited power generating units like fuel cells and battery to achieve the required near zero emission. A highly efficient aerodynamic body structure is required for the vehicle to reduce drag force and power consumption. Fuel cell powered vehicles offer technical and commercial advantages without compromising safety measures associated with fuel storage onboard vehicle. Hoffrichter et al [1] studied the performance of a hydrogen-hybrid railway traction vehicle 'Hydrogen Pioneer'. The observed overall duty cycle efficiency of the power-plant was from 28% to 40%. The peak-power demand was provided by the battery-pack, while average power during the duty cycle was met by the fuel cell stack. Bradley et al [2] compared the performance of a fuel cell powered unmanned aircraft's power plant with other 0.5-1 kW fuel cell power plants in the literature. The unmanned aircraft featured a 500 W polymer electrolyte membrane fuel cell with full balance of plant and compressed hydrogen storage incorporated into a custom airframe.

Yadav and Verma [3] simulated the design of a modern hydrogen fuel cell vehicle having fuel cell stack providing maximum 400 volts supply using 400 fuel cells. They found that fuel cell did not give frequent backup during the changes in speed but this drawback of fuel cell is compensated by additional energy provided by the battery. Bang et al [4] modelled a fuel cell powered electric vehicle consisting of a proton exchange membrane (PEM) fuel cell stack and balance of plant (BOP) along with a commercial vehicle simulation

program. Blower type and compressor type air feeding systems were modeled by using MATLAB/Simulink environment and the effect of fuel cell stack size (number of cells and cell area) on the fuel economy and performance of the fuel cell powered vehicle was investigated. Dincer [5] presented the hydrogen energy-utilization patterns for better environment and sustainable development, and showed how the principles of thermodynamics via energy can be beneficially used to evaluate hydrogen and fuel cell systems and their role in sustainability.

Ogden et al [6] compared compressed gas hydrogen storage, steam reforming of methanol and partial oxidation (POX) of hydrocarbon fuels derived from crude oil as three leading options for fuel storage onboard fuel cell vehicles. Manish and Banerjee [7] compared petrol driven internal combustion (IC) engine, compressed natural gas driven IC engine, compressed hydrogen storage and metal hydride (FeTi) storage based on PEM fuel cells as alternative vehicle technologies for a typical small family car in India (Maruti 800). Each technology option was simulated in MATLAB using a backward facing algorithm to calculate the force and power requirement for Indian urban drive cycle. They found that the CO<sub>2</sub> emissions were lowest for the fuel cell vehicle with compressed hydrogen storage (98 g/km) as compared to the petrol vehicle (162 g/km).

The present research envisages design, analysis and optimisation of an ultra-fuel efficient prototype vehicle to participate in Shell Eco Marathon Asia competition. As per the rules and regulations of the competition, the challenge was to design and build a hydrogen fuel cell powered prototype vehicle with an aerodynamic body

and three wheels. The concept was to design the vehicle with gullwing doors to resemble the unfrozen wings of a hawk. Computational Fluid Dynamics (CFD) is utilized as a tool for predicting and analysing fluid flow across the body. CFD allows optimizing the design based on flow dynamics, heat transfer, and pressures without having to build a large number of prototypes. This paper presents design, analysis and development of a highly aerodynamic and a near zero emission single seater three wheeler Unfrozen Hawk prototype vehicle that is powered by hydrogen fuel cell. The vehicle is designed with a tadpole configuration and gullwing doors to achieve low drag and a streamlined half body. The pressure and velocity distribution with an optimal value of drag coefficient are established using CFD analysis. The hydrogen consumption and heat generated in the fuel cell & Brushless Direct Current (BLDC) motor are analyzed for various cases.

## 2. Vehicle structure & system design

The unfrozen hawk vehicle design consists of main frame in tadpole configuration with three wheels and an aerodynamic outer body. The vehicle consists of a front compartment for driver and rear compartment for power train and fuel cell. Gullwing doors are provided for driver compartment. For proper ventilation of rear compartment, vents and openings are provided on the body. The frame structure composed of aluminium alloy 6061-T6 [8] tubes having mechanical properties as given in Table 1. The outer body is designed to minimize the drag coefficient while resembling the unfrozen wings when the doors are opened. The outer aerodynamic body is composed of light weight Glass Fibre Reinforced Plastic (GFRP) having low skin friction drag. The body and frame combine to make a sturdy and structurally safe aerodynamic shell.

**Table 1: Material properties of Aluminium alloy 6061-T6**

Properties	Al 6061-T6
Ultimate tensile strength, psi	32000
Yield strength, psi	28000
Brinell Hardness	71
Density, g/cc	2.7

Aerodynamic drag is defined as the longitudinal force resulting from the air flow past the vehicle body. The pressure drag and skin friction account for the aerodynamic drag of a vehicle. The coefficient of drag ( $C_d$ ) is defined as,

$$C_d = \frac{F_d}{0.5\rho V^2 A} \quad (1)$$

Where  $F_d$  is the drag force,  $\rho$  is the density of the fluid flowing past the body,  $V$  is the free stream fluid velocity and  $A$  is the projected cross sectional area of the body. The overall frontal area is largely a function of driver position and visibility requirements. Fig. 1 shows the variation of frontal area as a function of the seat back angle for a uniform width of 0.6 m to account for the driver's shoulders width and a high density foam side bolster. A vector diagram of the proposed driving position meeting driver's comfort and overall height requirements is shown in Fig. 2.

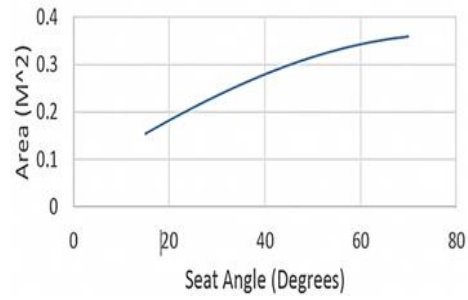


**Fig. 1: Variation of frontal area vs. Seat back angle**

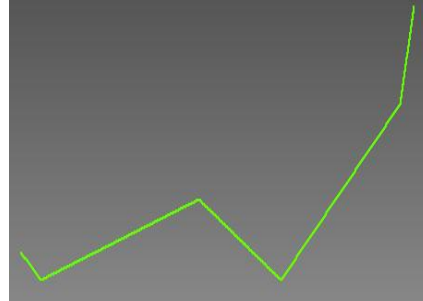


**Fig. 2: Driving position selected for design**

The drag force is calculated using Eqn. (1) over a range of frontal areas to see the effects of drag force over the entire vehicle speed range as shown in Fig. 3. The coefficient of drag ( $C_d$ ) is initially set to 0.15 which is the standard for a streamlined half body with wheels. With an optimized selection of visibility criteria, driver comfort and drag force, the surface modelling is undertaken using Autodesk Inventor software [9] with cross sectional curves as shown in Fig. 4 to provide a minimized overall frontal area of 1.82 m<sup>2</sup> in final design. Different views of the designed vehicle are shown in Fig. 5. The wheel base length and track width are 2.4m and 1.5 mm. An optimum back-rest angle of 50° provides the aerodynamic design of vehicle's body.

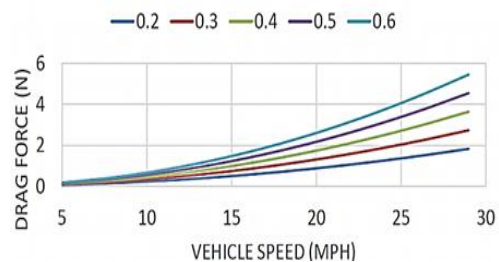


**Fig. 3: Drag force vs. Vehicle speed for variation of  $C_d$**

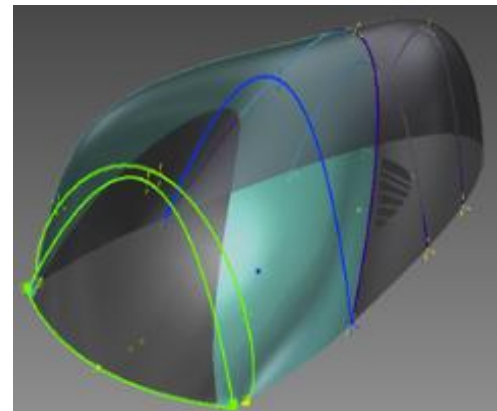


**Fig. 4: Surface modelling of vehicle body**

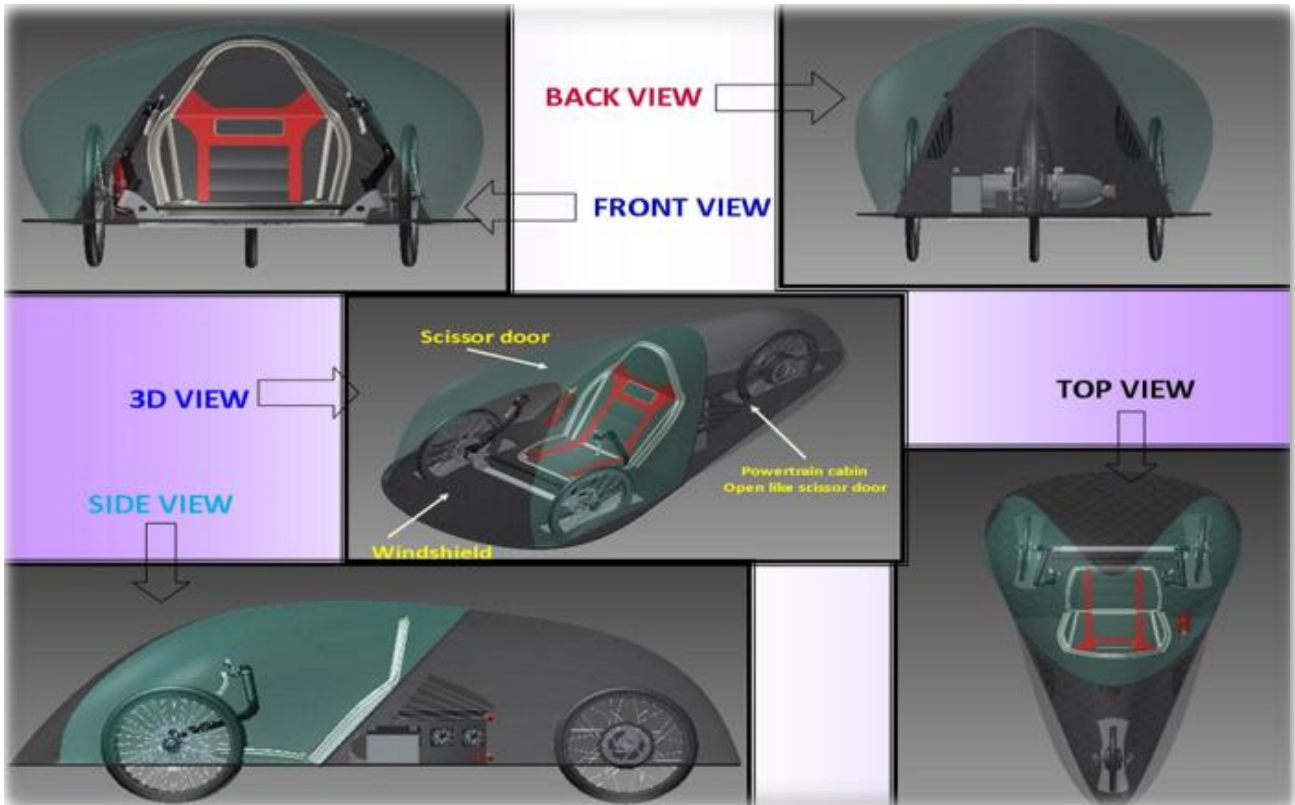


Fig. 5: Standard views of designed vehicle structure & system

### 3. CFD simulation for vehicle body

The vehicle design is analysed for aerodynamic performance [10] using CFD utilities in Autodesk flow design software. The tool is used to simulate and visualize the flow pattern, velocity distribution, pressure distribution and drag curves over the vehicle surface. The final design is simulated with initial parameters of wind speed of 2 m/s and frontal area of 1.82 m<sup>2</sup>. The aerodynamic performance is then visualized by incrementing the wind speed by 2 m/s per increment up to 10 m/s. Table 2 summarises the key results from the CFD simulations. Figs. 6 and 7 show the velocity and pressure distribution at the different velocity. For simulations at various wind speeds, the  $C_d$  remained more or less constant. The average value of  $C_d$  is coming out to be 0.352. The drag force increases with wind speed for an almost constant value of  $C_d$ . As expected, the maximum values of velocity and pressure have increased when wind speed is increased. CFD simulation has helped to improve the sustainability of a vehicle, for which the coefficient of drag can be selected as per the target fuel consumption. The unfrozen hawk prototype vehicle manufactured is shown in Fig. 8.

Table 2: Vehicle aerodynamics performance

Wind speed (m/s)	Drag force (N)	Drag coeff.	Max. velocity (m/s)	Max. pressure (Pa)
2	6.356	0.34	3.8	2.40
4	6.356	0.35	7.6	10.09
6	14.09	0.36	11.385	29.104
8	24.889	0.36	15.177	53.33
10	32.219	0.35	18.973	81.735

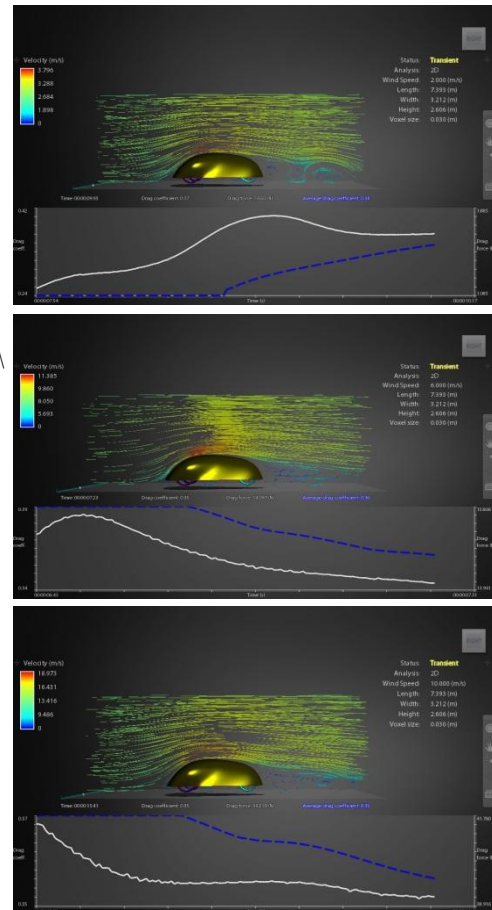


Fig. 6: Velocity distribution at 2 m/s (top), 6 m/s (middle) and 10 m/s (bottom)

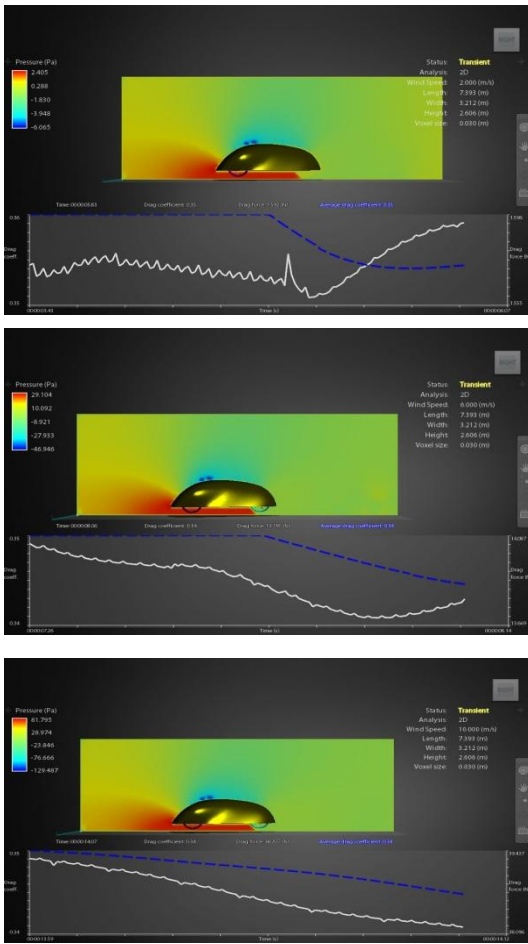


Fig. 7: Pressure distribution at 2 m/s (top), 6 m/s (middle) and 10 m/s (bottom)



Fig. 8: Unfrozen hawk prototype vehicle

#### 4. Heat generation in fuel cell and motor

Fuel cells are a family of technologies that generate electricity through electrochemical process. A PEM fuel cell is a device that converts hydrogen and oxygen into water and electricity. The H-1000XP fuel cell stack used in unfrozen hawk is a cathode-cooled PEM fuel cell stack designed to provide stable electrical power while operating on air and dry hydrogen. The hydrogen fuel cell is used as the power source for driving the BLDC motor [11] on the rear wheel of vehicle. The specifications of fuel cell are given in. Table 3.

Table 3: Fuel cell specification

Parameter	Value
Peak power	1.1 kW
Rated current	0-33.5A at 30V
DC voltage	25V - 48V
Reactants	Hydrogen and Air
Composition	99.99% dry H <sub>2</sub>
H <sub>2</sub> pressure	7.2 - 9.4 psi
Hydrogen consumption at 1 kW	13.5 SPLM

The heat generated in single cell ( $q$ ) is given by,

$$q = P(1/\eta - 1) \tag{2}$$

Where  $P$  is the power produced by a single cell which is a product of current and cell voltage as,

$$P = IVc \tag{3}$$

The low heat value efficiency ( $\eta$ ) is given by,

$$\eta = Vc/1.25 \tag{4}$$

Total heat generated in a fuel cell is given by,

$$Q = Nq \tag{5}$$

Where  $N$  is total number of cells in a fuel cell stack. For a commercial fuel cell stack with  $Vc = 0.96V$  and  $N = 50$ , the heat generated in the fuel cell for various current input is given in Table 4. The value of  $\eta = 76.8\%$ . The heat coefficient is  $65W/m^2-K$ . The internal and external temperature of the fuel cell is  $50^\circ C$  and  $20^\circ C$  respectively. The heat increases with respect to the speed of the vehicle. The average heat in fuel cell is 23 W.

Table 4: Generated heat in fuel cell for various input currents

I (Coulomb)	P (W)	q (W)	Q (W)
1.822	1.74912	0.5282	26.41
1.913	1.83648	0.5546	27.43
2.399	2.30304	0.6955	34.775
3.325	3.192	0.9639	48.19
4.728	4.538888	1.370	68.5
6.735	6.4656	1.9526	97.63
9.035	8.6736	2.619	130.95
11.544	11.08	3.346	167.3
14.309	13.73	4.416	220.8

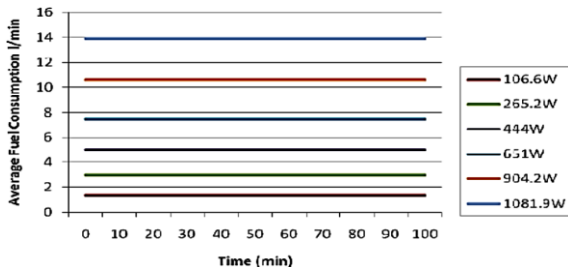
BLDC permanent magnet motors are increasingly being employed in electric vehicles and hybrid electric vehicles due to their high efficiency, high power density and minimal maintenance. BLDC motor has approx. 40% efficiency and remaining efficiency of the motor is lost [12]. The Lorentz force law shows that a motor can produce force from current. The current/voltage relationship shows that it can produce voltage from velocity. Power transfer in BLDC motor occurs when voltage, current, force and velocity are present at the same time. Electric 48V 1kW hub motor is used in the prototype vehicle where current varies and the voltage is kept constant. The heat losses associated with copper losses, iron losses and mechanical losses are only accounted in this analysis. The difference between input and output power is used to evaluate the direct heat loss. The dissipated heat in BLDC motor with respect to the variation of the current is given in Table 5.

**Table 5: Dissipated heat in BLDC motor**

Current (Coulomb)	Input power (W)	Output power (W)	Heat loss (W)
1.822	88.24	21.25	66.99
1.913	92.65	8.95	83.7
2.399	116.18	40.54	75.67
3.325	161.03	78.32	82.71
4.728	228.98	161.86	67.12
6.735	326.18	258.13	68.05
9.035	437.57	361.13	75.75
11.544	559.08	447.49	111.59
14.309	692.98	579.72	113.26

## 5. Fuel consumption analysis

The average fuel consumption at different load condition with respect to time is shown in Fig. 9. The prototype vehicle is tested for fuel consumption [13] with and without the attachment of the aerodynamic vehicle body. The vehicle is run for two minutes at maximum throttle (30 kmph) and fuel consumption is recorded each time for different cases using thermal mass flow meters for hydrogen gas. For both situations of vehicle body, the cylinder pressure and stack input pressure are kept as 1.25 kg/cm<sup>2</sup> and 7.25 psi respectively. The results are summarised in Table 6. The average hydrogen consumption with and without body attachment is 4.95 l and 7.82 l respectively resulting in a 36.7% reduction in fuel consumption due to aerodynamic vehicle body.

**Fig. 9: Average fuel consumption (l/min) vs. Load (W)****Table 6: Fuel consumption test run results**

Situation/ Cases	Hydrogen flow meter reading (l)		
	Initial	Final	Consumption
Vehicle without aerodynamic body	62.04	69.56	7.52
	70.32	78.44	8.12
	81.71	88.99	7.82
With aerodynamic body	89.77	94.33	4.56
	95.02	99.89	4.87
	101.02	106.44	5.42

## 6. Conclusion

The eco-friendly behaviour of the unfrozen hawk vehicle is enhanced by employing the concept of aerodynamics and fuel consumption analysis together from design to fabrication of prototype. The role of CFD is well played by the tools to predict, simulate and visualize the flow across the body. The simulation of pressure and velocity distribution across the surface is an effective tool for further study and optimization of the outer body design. The presented research validated the role of aerodynamics for enhancing the energy efficiency of

green vehicles. We observed different kinds of fuel cell & motor heat losses internally and externally. The design can be further improved by addressing crashworthiness and overcoming heat losses.

## REFERENCES:

- [1] A. Hoffrichter, P. Fisher, J. Tutchter, S. Hillmansen and C. Roberts. 2014. Performance evaluation of the hydrogen-powered prototype locomotive 'Hydrogen Pioneer', *J. Power Sources*, 250, 120-127. <http://dx.doi.org/10.1016/j.jpowsour.2013.10.134>.
- [2] T.H. Bradley, B.A. Moffitt, D.N. Mavris, D.E. Parekh. 2007. Development and experimental characterization of a fuel cell powered aircraft, *J. Power Sources*, 171, 793-801. <http://dx.doi.org/10.1016/j.jpowsour.2007.06.215>.
- [3] G. Yadav and V. Verma. 2013. Design and performance analysis of hydrogen powered fuel cell vehicle, *Progress in Science and Engg. Research J.*, 2(03/06), 249-254.
- [4] J. Bang, H-S. Kim, D-H. Lee and K. Min. 2008. Study on operating characteristics of fuel cell powered electric vehicle with different air feeding systems, *J. Mechanical Science and Technology*, 22, 1602-1611. <http://dx.doi.org/10.1007/s12206-008-0417-6>.
- [5] I. Dincer. 2008. Hydrogen and fuel cell technologies for sustainable future, *Jordan J. Mechanical and Industrial Engineering*, 2(1), 1-14.
- [6] J. Ogden, M. Steinbugler and T. Kreutz. 1997. Hydrogen as a fuel for fuel cell vehicles: A technical and economic comparison, *Proc. 8<sup>th</sup> Annual Conf. National Hydrogen Association*, Arlington, USA.
- [7] S. Manish and R. Banerjee. 2006. Techno-economic assessment of fuel cell vehicles for India, *Proc. World Hydrogen Energy Conf.*, Lyon, France.
- [8] C.F. Tan and M.R. Said. 2009. Effect of hardness test on precipitation hardening Aluminium alloy 6061-T6, *Chiang Mai J. Sci.*, 36(3), 276-286.
- [9] Autodesk Inventor Software, <http://www.autodesk.com/>
- [10] N.T. Frink, M. Tormalm and S. Schmidt. Unstructured CFD aerodynamic analysis of a generic UCAV configuration, *PAPER NBR-25*, RTO-MP-AVT-170.
- [11] J. Kuria and P. Hwang. Investigation of thermal performance of electric vehicle BLDC motor, *Int. J. Mech. Engg.*, 1(1), 1-17.
- [12] J.C. Gamazo-Real, E. Vazquez-Sanchez and J. Gomez-Gil. 2010. Position and speed control of brushless DC motors using sensorless techniques and application trends, *Sensors*, 10(7), 6901-6947. <http://dx.doi.org/10.3390/s100706901>.
- [13] M.R.B. Mustaff, W.A.N.B.W. Mohamed and R.B. Atan. 2012. Analytical approach to predict hydrogen consumption of a lightweight PEM fuel cell vehicle, *Proc. IEEE Int. Conf. Control System, Computing and Engineering*, 489-494. <http://dx.doi.org/10.1109/iccsce.2012.6487195>.

## EDITORIAL NOTES:

*Edited paper from International Conference on Newest Drift in Mechanical Engineering, 20-21 December 2014, Mullana, Ambala, India.*

*GUEST EDITOR: Dr. R.C. Sharma, Dept. of Mech. Engg., Maharishi Markandeshwar University, Mullana, India.*